Letters

Complete ZVS Analysis in Dual Active Bridge

Yu Yan, *Student Member, IEEE*, Handong Gui, *Student Member, IEEE*, and Hua Bai, *Senior Member, IEEE*

***Abstract*—Zero-voltage-switching (ZVS) has been widely applied in widebandgap devices based on high-switching-frequency converters, for instance, dual-active-bridge isolated dc–dc converter, which consists of two H-bridges. To secure ZVS for all eight switches, previous literature mostly focuses on half-bridge to analyze switching transitions, which, however, is rather incomplete due to ignoring the impact of modulation strategies and cannot fulfill all circumstances. In this letter, the whole H-bridge is used as a unit to analyze the ZVS transient process, addressing the ZVS setting in different modulation strategies. The minimal initial inductor energy to complete the ZVS process is also quantified, which in return can reduce the transformer current, thereby enhancing the efficiency. Furthermore, the accurate ZVS transition time is derived incorporating with the nonlinearity of switch output capacitance, which can be further used to set the dead-band time. An H-bridge prototype with SiC devices is built up to verify the theory proposed in this letter.**

***Index Terms*—Dual-active bridge (DAB), H-bridge, output capacitor, phase shift control, zero-voltage-switching (ZVS).**

I. Introduction

How to realize zero-voltage-switching (ZVS) in a dual-active-bridge (DAB) application has been discussed in early literature [1]. Including single-phase shift (SPS), dual-phase shift (DPS), triple-phase shift (TPS), and multiphase shift (MPS), various modulation strategies have been proposed to achieve ZVS in full-load and wide-voltage range [2]–[4]. To analyze the detailed ZVS process during the dead band, an H-bridge circuit is extracted out of DAB in Fig. 1(a), as shown in (b), where V_{in} is the input voltage source and V_s is the reflected secondary-side voltage, which can be $+nV_o$, $-nV_o$, or zero according to the secondary-side modulation. Because of the symmetry of DAB structure, analyzing one side, saying primary-side H-bridge, is sufficient. Note that achieving ZVS relies on the resonance [5], [6] between the transformer leakage inductance L and switch output capacitance C_{oss}. But the resonant loop can be totally different under different modulation strategies, which, however, has been ignored in the previous analysis [5]–[8]. Some literature [7], [8] proposed the equivalent capacitance based on the half-bridge model, where the charge-based, energy-based, or other types of equivalent capacitance are employed for different purposes. But the proper derivation of ZVS transition time with the consideration of different modulation strategies has not been addressed yet. In [9], the parasitic parameters of the transformer are further considered, when it is comparable with switch C_{oss}.

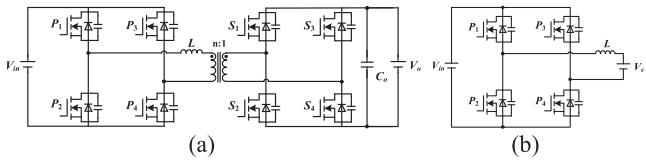

Fig. 1. Topology. (a) DAB. (b) Simplified circuit for ZVS analysis based on H-bridge.

To achieve ZVS in real converters, two essential parameters should be carefully selected, i.e., the initial inductor energy and the dead-band time. Increasing the initial inductor current helps ZVS realization, which, however, serves as reactive power and reduces efficiency [4], [10]. Similarly, longer dead-band time guarantees the completion of ZVS but increases loss because of the increased body-diode conduction time. To achieve optimal performance, it is important to calculate the required initial energy and ZVS transition time accurately in all circumstances, which is lacking in the present studies. So, this letter introduces an analytical method to accurately estimate the ZVS transient process in DAB, addressing minimum required leakage inductor energy and ZVS transition time in different modulation strategies. The nonlinear C_{oss} of one leg in the transient process is reconsidered in Section II. The detailed ZVS transient process without and with the inner phase shift is modeled in Sections III and IV, respectively. The analytical results are compared with experimental results in Section V. Finally, Section VI gives the conclusion.

II. Precalculation of Charge and Energy

The ZVS process of one leg is shown in Fig. 2(a). In the transition process, the C_{oss} of complementary switches gets charged and discharged, simultaneously. The energy exchange during ZVS realization happens among inductor, C_{oss}, input voltage source V_{in}, and reflected output voltage source V_s. To quantify such exchanged energy accurately, the charge flowing through

Manuscript received May 7, 2020; revised June 8, 2020 and July 1, 2020; accepted July 19, 2020. Date of publication July 23, 2020; date of current version September 22, 2020. *(Corresponding author: Yu Yan.)*

The authors are with the Department of Electrical Engineering and Computer Science, University of Tennessee, Knoxville, TN 37996 USA (e-mail: yyan15@vols.utk.edu; hgui@vols.utk.edu; kevinbai@icloud.com).

Color versions of one or more of the figures in this letter are available online at https://ieeexplore.ieee.org.

Digital Object Identifier 10.1109/TPEL.2020.3011470

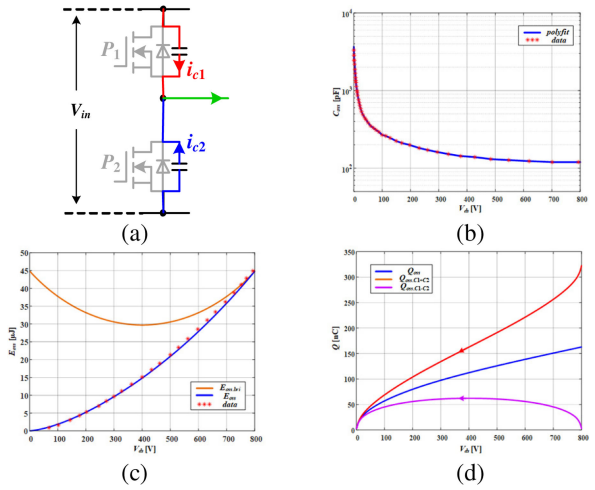

Fig. 2. Characteristics of nonlinear output capacitance in one bridge leg. (a) ZVS transition. (b) $C_{\rm oss}$. (c) $E_{\rm oss}$. (d) $Q_{\rm oss}$.

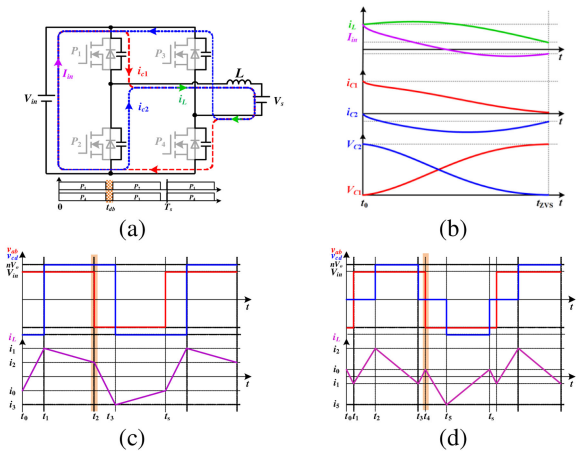

Fig. 3. H-bridge ZVS transient process without the inner phase shift. (a) Transient process. (b) Transient process waveforms. (c) SPS. (d) DPS.

the inductor, the voltage sources, and the charge remained in $C_{\rm oss}$, all need to be mathematically formulated.

Curve fitting is usually used by referring to data points from the switch datasheet. For instance, Fig. 2(b) shows $C_{\rm oss}$ created by the interpolant method using the original data points from the datasheet of SCT3030KL [11]. The $E_{\rm oss}$ curve is then calculated based on the $C_{\rm oss}$ curve, as shown in Fig. 2(c), which is compared with the data imported from the datasheet. This then allows us to calculate the stored energy of one leg in the ZVS process with the 800 V input voltage, as shown by the orange curve. The charge stored in $C_{\rm oss}$ is shown by the blue curve in Fig. 2(d), which is calculated based on the $C_{\rm oss}$ curve. Note that the x-axis is $V_{\rm ds}$ of the bottom switch P_2. The charge flowing out/in the bridge middle point is the red curve in Fig. 2(d), which is the sum of the charge flowing through two switches. The difference between the charges flowing through two switches is the purple curve. The data presented in Fig. 2(c) and (d) will then be utilized to estimate the ZVS transient process in the following sections. Switch P_2 will be used as an example to analyze the ZVS process in different conditions. If the parasitic capacitance between drain and source is comparable with $C_{\rm oss}$, it should be included when fitting the curve to ensure the accurate estimation.

III. Modulation Without Inner Phase Shift

Considering the primary H-bridge without the inner phase shift, P_1 and P_4 switch ON and OFF at the same time. In this case, $C_{\rm oss}$ of P_1 and P_4 are charged or discharged simultaneously with the same $V_{\rm ds}$ value. The input and output voltage sources, four switch capacitances, and the inductor participate in the resonant process. However, the existing half-bridge analysis cannot describe the true resonant loop, leading to an inaccurate calculation of minimal inductor energy. Fig. 3(a) illustrates the real ZVS transient process with the control scheme shown in Fig. 3(c) and (d). Time intervals in shadow represent the transient in Fig. 3(a). The current flowing through switches is shown in Fig. 3(b).

Such a ZVS transient process happens when P_1 and P_4 are switched OFF, while P_2 and P_3 are not ON yet. In the beginning, the current flows out of the input voltage source, and $V_{\rm in}$ supplies the power for the ZVS process. But the polarity of the current is gradually reversed, indicating that the $V_{\rm in}$ is beginning to consume energy. Actually, the power supplied or dissipated by the input voltage source is zero, although such input voltage source influences the ZVS transition time, as derived later.

Assuming the voltage across the output capacitance of P_1 is v, the relationship between the capacitance-voltage and inductor-current is shown in the following equations:

$$\begin{cases} V_{\rm in} = V_{C1}(t) + V_{C2}(t) \\ v = V_{C1}(t) \end{cases} \tag{1}$$

$$\begin{cases} i_{\rm in}(v) = i_{C1}(v) - i_{C2}(V_{\rm in} - v) \\ i_L(v) = i_{C1}(v) + i_{C2}(V_{\rm in} - v) \\ i_{C1}(v) = C_1(v)\frac{dv}{dt} \\ i_{C2}(v) = -C_2(V_{\rm in} - v)\frac{d(V_{\rm in}-v)}{dt}. \end{cases} \tag{2}$$

To get the power consumed by the voltage source in the circuit, the charge flowing through the inductor and dc source in the transient process is needed, which is

$$\begin{cases} Q_{i_L}(v) = \int_0^v (C_1(v) + C_2(V_{\rm in} - v))dv \\ Q_{i_{\rm in}}(v) = \int_0^v (C_1(v) - C_2(V_{\rm in} - v))dv. \end{cases} \tag{3}$$

So, the energy dissipated in the input and the output voltage sources in the transient process is

$$E_{\rm diss}(v) = -Q_{i_{\rm in}}(v)V_{\rm in} + Q_{i_L}(v)V_s. \tag{4}$$

The total initial energy stored in the inductor and the H-bridge is

$$E_{\rm init} = \frac{1}{2}Li_L^2(0) + 2E_{\rm oss.bri}(0). \tag{5}$$

The remaining energy in the H-bridge and the inductor at the end of ZVS is

$$E(v) = \frac{1}{2}Li_L^2(v) + 2E_{\rm oss.bri}(v) = E_{\rm init} - E_{\rm diss}(v). \tag{6}$$

Combining (4)–(6), the inductor current can be derived based on the certain capacitor voltage, which is

For the ZVS transition time, we need to simplify (1) and (2) to get the relationship between v and inductor current as

$$\frac{(C_1(v)+C_2(V_{\rm in}-v))dv}{i_L(v)}=dt. \tag{8}$$

Based on (7), as shown at the bottom of this page, the inductor current can also be expressed as a function of v. In the transient process, the output capacitance of P_1 is charged. So v increases from zero to $V_{\rm in}$, and the transition time increases from zero to $t_{\rm ZVS}$. Then

$$t_{\rm ZVS}=\int_0^{t_{\rm ZVS}}dt=\int_0^{V_{\rm in}}\frac{(C_1(v)+C_2(V_{\rm in}-v))}{i_L(v)}dv. \tag{9}$$

During the whole transient process, the charge flowing through $C1$ and $C2$ are the same. So, according to (3), the total charge flows through the input voltage source is zero, as shown in the following:

$$\begin{cases}\int_0^{V_{\rm in}}Q_{\rm in}(v)dv=0\\ E_{\rm oss.bri}(0)=E_{\rm oss.bri}(V_{\rm in}).\end{cases} \tag{10}$$

Thus, the only energy exchange in the whole ZVS process without the inner phase happens between the inductor and the output voltage source. To complete the ZVS transient process, the minimum inductor energy is

$$\frac{1}{2}Li_L^2(0)\geq 2Q_{\rm oss}(V_{\rm in})V_s. \tag{11}$$

If half-bridge is used to analyze the transient process, the input voltage source may also dissipate or supply power, which results in overestimation or underestimation of the required energy. To accurately estimate the ZVS transition time, the instantaneous capacitance of the H-bridge instead of a constant equivalent capacitance should be considered, along with the interaction with the input voltage source, even though $V_{\rm in}$ does not contribute any energy.

IV. Modulation With Inner Phase Shift

In SPS modulation, the pure square waveform with a 50% duty cycle at the primary or the secondary side is the simplest way to regulate the power. When the voltage gain is far away from one or at light load, DAB can lose ZVS easily. Many modulation strategies [2], [3] adopt the inner phase shift to extend the ZVS range, such as DPS, TPS, and MPS. These modulation strategies yield a three-level waveform with different ZVS settings. In this case, only two of switch output capacitances participate in the resonant process. A switch in the other leg provides the bypass for the inductor current, which makes the current flowing through the input and the output voltage sources differently. The resonant loop with the inner phase shift is different from the loop discussed in Section III.

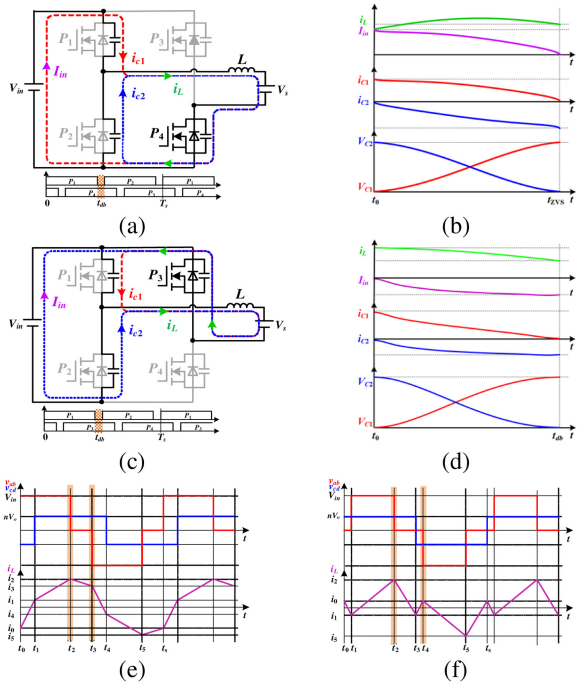

Fig. 4. H-bridge ZVS transient process with inner phase shift. (a) Transient process. (b) Transient process waveform. (c) Implementation in SPS. (d) Implementation in DPS. (e) and (f) Examples for DPS.

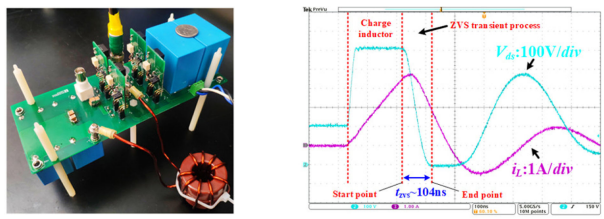

Fig. 5. Experimental validation. (a) H-bridge prototype. (b) Switching waveform.

In Fig. 4(a) and (c), the ZVS transient processes for the lower switch P_2 happens with an inner phase shift added at the primary side. Fig. 4(e) and (f) shows the related waveforms. Fig. 5(a) corresponds to $t=t_2$ in Fig. 4(e) and (f). Fig. 4(c) is for $t=t_3$ in Fig. 4(e), and $t=t_4$ in Fig. 4(f).

In Fig. 4(a), the current flowing through the input voltage source is the same as the charging current of C_1

$$Q_{\rm in}(v)=\int_0^v C_1(v)dv. \tag{12}$$

Different from the SPS control, where all four switch capacitances are involved, here only two capacitances in one leg participate in the transient. The relationship between the inductor

$$i_L(v)=\sqrt{i_L^2(0)+\frac{2}{L}(2E_{\rm oss.bri}(0)-2E_{\rm oss.bri}(v)-Q_{i_L}(v)V_s+Q_{i_{\rm in}}(v)V_{\rm in})}. \tag{7}$$

current and the voltage across P_1 can be written as (13), as shown at the bottom of this page.

Equation (9) can still be used to estimate the time interval to realize ZVS. But from the energy point of view, the input voltage source supplies the energy and the output voltage source consumes the energy. In this case, the minimal energy stored in the inductor to complete the ZVS transient process is

$$\frac{1}{2}Li_L^2(0) \geq 2Q_{\rm oss}(V_{\rm in})V_s - Q_{\rm oss}(V_{\rm in})V_{\rm in}. \tag{14}$$

For the transient process shown in Fig. 4(c), the charge flowing through the input voltage source is

$$Q_{\rm in}(v) = -\int_0^v C_2(V_{\rm in} - v)dv. \tag{15}$$

In this circumstance, the input and output voltage sources consume the energy from the inductor. So the minimal inductor energy to ensure ZVS is

$$\frac{1}{2}Li_L^2(0) \geq 2Q_{\rm oss}(V_{\rm in})V_s + Q_{\rm oss}(V_{\rm in})V_{\rm in}. \tag{16}$$

where $V_{\rm s}$ can be positive, zero, or negative, depending on the modulation strategies at the transformer secondary side.

As a summary, compared with the situation without the inner phase shift, the input voltage source affects not only the ZVS transition time but also the minimum required initial energy stored in the inductor. For the different combinations of switching actions, $V_{\rm in}$ can dissipate or supply energy, which should be given full consideration in different modulation strategies. V_s still influence the ZVS process, as discussed in Section III.

V. Experiment Verification and Comparison

A. Experiment Verification

To verify the ZVS transient process formulated earlier, an H-bridge prototype shown in Fig. 5 has been built. The parameters are presented in Table I. The reflected secondary side voltage is replaced with a dc power supply. $V_{\rm ds}$ of the bottom switch P_2 and the inductor current are measured, which can indicate the energy exchange during the switching transient. Fig. 5(b) shows an exemplary experimental waveform. Based on the measurement data, an *I–V* curve is plotted with the ZVS transition time calculation. Such an experimental *I–V* curve is then compared with the estimated curve resulted from (7) and (14) to verify the energy exchange in the proposed analysis. The estimated and experimental ZVS transition time are listed in Table II, which shows a good match.

Fig. 6 shows the experimental results of the ZVS transient process based on the modulation without the inner phase shift at the primary side. The input voltage, output voltage, and the initial inductor current are provided in the corresponding figures. All the calculated *I–V* curves are overlapped with experimental results. When the output voltage $V_s = 0$, there is no energy dissipated in the transient process, i.e., the initial and final inductor current values remain nearly the same.

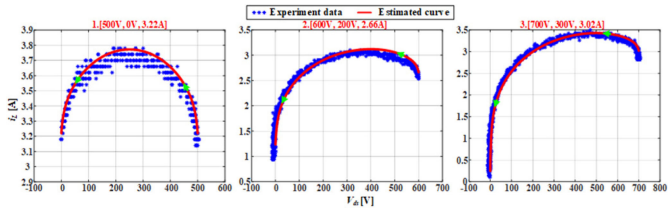

Fig. 6. *I–V* curve comparison based on the modulation without inner phase shift at [$V_{\rm in}$, V_s, $i_L(0)$].

TABLE I
Prototype Setup

Name	Value	Name	Value
Switch	SCT3030KL	Inductor	20μH
Scope	MDO4104C	Voltage probe	TPP0805
Current probe	TCP0030		

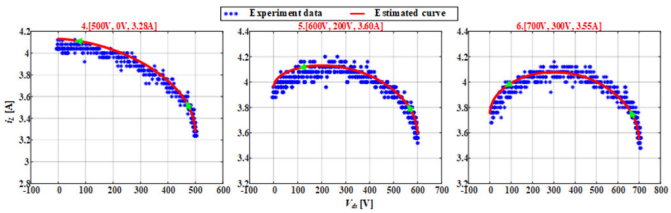

Fig. 7. *I–V* curve comparison based on the modulation with inner phase shift-lower switch ZVS at [$V_{\rm in}$, V_s, $i_L(0)$].

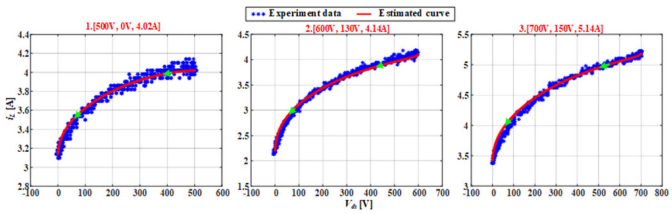

Fig. 8. *I–V* curve comparison based on the modulation without inner phase shift-upper switch ZVS at [$V_{\rm in}$, V_s, $i_L(0)$].

For the modulation with the inner phase shift, Fig. 7 shows the test results related to Fig. 4(a). Here $V_{\rm in}$ supplies the energy to help complete the ZVS process. So i_L may increase in the transient process. Test results are consistent with the estimation.

The test results shown in Fig. 8 correspond to Fig. 4(c). In this case, P_2 is also discharged in the transient process, and $V_{\rm in}$ consumes energy. According to Fig. 8, the estimated and experimental *I–V* curves are still well aligned.

$$i_L(v) = \sqrt{i_L^2(0) + \frac{2}{L}(E_{\rm oss.bri}(0) - E_{\rm oss.bri}(v) - Q_{i_L}(v)V_s + Q_{i_{\rm in}}(v)V_{\rm in})} \tag{13}$$

TABLE II
TRANSITION TIME COMPARISON

(ns)\#	1	2	3	4	5	6	7	8	9
Estimation	70.5	106.8	121.3	65.2	69.5	76.1	67.23	80.44	66.62
Experiment	71.4	104	118.3	65.8	69	77.8	69.6	84.2	71

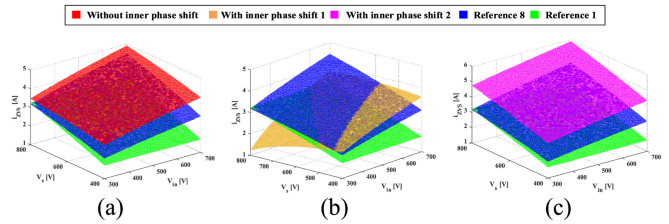

Fig. 9. Comparison of minimal initial inductor current. (a) Without inner phase shift. (b) With inner phase shift 1. (c) With inner phase shift 2.

TABLE III
COMPARISON OF MINIMUM INITIAL INDUCTOR ENERGY

Modulation	Minimum initial inductor current Equation	Value
Without inner phase shift	$\frac{1}{2}Li_L^2(0) \geq 2Q_{oss}(V_{in})V_s$	110.86μJ
With inner phase shift 1	$\frac{1}{2}Li_L^2(0) \geq 2Q_{oss}(V_{in})V_s - Q_{oss}(V_{in})V_{in}$	29.52μJ
With inner phase shift 2	$\frac{1}{2}Li_L^2(0) \geq 2Q_{oss}(V_{in})V_s + Q_{oss}(V_{in})V_{in}$	192.21μJ
Reference [1]	$\frac{1}{2}Li_L^2(0) \geq 2CV_{in}nV_o$	59.66μJ
Reference [8]	$\frac{1}{2}Li_L^2(0) \geq Q_{oss}(V_{in})V_{in}$	83.15μJ

Note: 1) "C" in [1] is simplified $C_{\rm oss}$; 2) $Q_{\rm oss}(600\ {\rm V}) = 138.58$ nQ.

B. Comparison and Improvement

Based on the analysis in Sections III and IV, the minimum initial inductor current depends on the different modulation strategies, which is categorized in Table III. An example of the detailed values based on $V_{\rm in} = 600$ V and $V_s = 400$ V in different circumstances is also presented in the table. It is observed that the calculations in references based on a single half-bridge are not accurate. The comparisons of minimum initial current to fully realize ZVS within a certain input and output voltage ranges are shown in Fig. 9. The previous ZVS analysis cannot fulfill all circumstances, which can cause either underestimation or overestimation. In the following section, an example is provided to address the general concern about ZVS realization, e.g., efficiency and stability.

Based on switches used in the experiment, the influence of an inaccurate ZVS setting can be estimated at the converter level. Here is the example. The key parameters of the converter are presented in Table IV. For DAB, DPS, and TPS are usually used at a medium or light load to realize ZVS and improve efficiency, while for IGBTs ZCS is also a good choice [12]. The switching waveform, as shown in Fig. 4(f), is a kind of TPS modulation, which can realize ZVS and lower current stress [3], [4]. The power range to implement this TPS control is 0–2 kW. The primary H-bridge has the inner phase shift and the secondary H-bridge does not. In the half switching cycle, there are three switching actions. At t_1, the ZVS transient process is corresponding to the resonant loop in Fig. 4(c). The inductor current at t_2 is the peak current in the switching period and easy to realize ZVS. The ZVS transient process at t_3 is corresponding to the resonant loop in Fig. 3(a) at the secondary side.

TABLE IV
SPECIFICATION OF DAB CONVERTER [3]

Input voltage	700V	Output voltage	340V
Switching frequency	100KHz	Turn ratio	2
Primary switch	SCT3030KL	Secondary switch	SCT3022AL
Paralleled switches	2	Maximum Power	18kW
Inductor	20μH		

For the transient process at t_1, the ZVS process happens at the primary side. The $Q_{\rm oss}$ (700 V) is 302 nC. According to (16), the required minimal initial inductor energy is 622 μJ, i.e., the inductor current at t_1 should be larger than 7.88 A to complete the ZVS process. According to [8], which only considers a single half-bridge model, the minimal initial inductor energy is 211.4 μJ, and the inductor current is 4.59 A. When the inductor current drops to zero, the voltage across $C_{\rm oss}$ is 411 V. The energy remained in $C_{\rm oss}$ will be dissipated when switches turn ON, which is 17 μJ in Fig. 2(c). The same analysis also applies to the secondary side, which will not be introduced in detail. The remaining energy in each $C_{\rm oss}$ at the secondary side is 8 μJ. The total switching-ON loss caused by the incomplete ZVS setting is 13.2 W. If operated at 1 kW, the efficiency decrement can be more than 1%.

The switching frequency in this example is 100 kHz. In other applications with lower power rating and higher switching frequency (up to MHz), the incomplete ZVS can have a more aggravated influence. This letter also provides the calculation of accurate ZVS transition time to set the proper dead-band time. With insufficient dead-band time, the ZVS process cannot be finished. If the dead-band time is too long, it can increase the conduction loss, and incur incomplete ZVS [3], which deteriorates the system reliability due to switch crosstalk [13].

VI. CONCLUSION

For DAB converters, previous literature does not consider the influence of modulation strategies, which can alter the resonant loop in ZVS transients. The simple half-bridge model used in existing literature cannot cover all cases. In this letter, three basic ZVS resonant loops based on the H-bridge model with different minimal initial inductor energy to fully realize ZVS are proposed, as the main contribution. The accuracy of the proposed analysis is verified experimentally. The comparison of *I–V* curves can be used to comprehend the energy exchange in the transient process, which helps to further verify the proposed minimal initial inductor energy. Based on this, considering the nonlinearity of switch output capacitance, this letter accurately derives the ZVS transition time by utilizing $C_{\rm oss}$ curve from the datasheet.

The proposed calculation of the minimal initial inductor energy and the transition time can be the accurate references to set ZVS current and dead-band time in real converter applications. With the proper inductor current for ZVS, the reactive power can also be limited, which helps to further improve the efficiency.

REFERENCES

[1] M. N. Kheraluwala, R. W. Gascoigne, D. M. Divan, and E. D. Baumann, "Performance characterization of a high-power dual active bridge dc-to-dc converter," *IEEE Trans. Ind. Appl.*, vol. 28, no. 6, pp. 1294–1301, Nov./Dec. 1992.

[2] G. Oggier, G. O. García, and A. R. Oliva, "Modulation strategy to operate the dual active bridge dc–dc converter under soft switching in the whole operating range," *IEEE Trans. Power Electron.*, vol. 26, no. 4, pp. 1228–1236, Apr. 2011.

[3] Y. Yan, H. Bai, A. Foote, and W. Wang, "Securing full-power-range zero-voltage switching in both steady-state and transient operations for a dual-active-bridge-based bidirectional electric vehicle charger," *IEEE Trans. Power Electron.*, vol. 35, no. 7, pp. 7506–7519, Jul. 2020.

[4] Z. Guo, "Modulation scheme of dual active bridge converter for seamless transitions in multiworking modes compromising ZVS and conduction loss," *IEEE Trans. Ind. Electron.*, vol. 67, no. 9, pp. 7399–7409, Sep. 2020.

[5] Texas Instruments, "Phase-shifted full-bridge, zero-voltage transition design considerations," Appl. Rep. SLUA107A, 2011.

[6] U. Kundu, K. Yenduri, and P. Sensarma, "Accurate ZVS analysis for magnetic design and efficiency improvement of full-bridge LLC resonant converter," *IEEE Trans. Power Electron.*, vol. 32, no. 3, pp. 1703–1706, Mar. 2017.

[7] D. Costinett, D. Maksimovic, and R. Zane, "Circuit-oriented treatment of nonlinear capacitances in switched-mode power supplies," *IEEE Trans. Power Electron.*, vol. 30, no. 2, pp. 985–995, Feb. 2015.

[8] M. Kasper, R. M. Burkart, G. Deboy, and J. W. Kolar, "ZVS of power MOSFETS revisited," *IEEE Trans. Power Electron.*, vol. 31, no. 12, pp. 8063–8067, Dec. 2016.

[9] Z. Zhang, Y. Xiao, M. A. E. Andersen, and K. Sun, "Impact on ZVS operation by splitting inductance to both sides of transformer for 1-MHz GaN based DAB converter," *IEEE Trans. Power Electron.*, vol. 35, no. 11, pp. 11988–12002, Nov. 2020, doi: 10.1109/TPEL.2020.2988638.

[10] B. Zhao, Q. Yu, and W. Sun, "Extended-phase-shift control of isolated bidirectional dc–dc converter for power distribution in microgrid," *IEEE Trans. Power Electron.*, vol. 27, no. 11, pp. 4667–4680, Nov. 2012.

[11] ROHM, "SCT3030KL Datasheet," 2018.

[12] T. Hirose, M. Takasaki, and Y. Ishizuka, "A power efficiency improvement technique for a bidirectional dual active bridge dc–dc converter at light load," *IEEE Trans. Ind. Appl.*, vol. 50, no. 6, pp. 4047–4055, Nov./Dec. 2014.

[13] Z. Zhang, F. Wang, L. M. Tolbert, and B. J. Blalock, "Active gate driver for crosstalk suppression of SiC devices in a phase-leg configuration," *IEEE Trans. Power Electron.*, vol. 29, no. 4, pp. 1986–1997, Apr. 2014.